Electronic Supplementary Material (ESI) for Chemical Communications.
This journal is © The Royal Society of Chemistry 2019

Electronic Supplementary Information

One-step MOF-derived Co/Co_9S_8 nanoparticles embedded in nitrogen, sulfur and oxygen ternary-doped porous carbon: efficient electrocatalyst for overall water splitting

Jiao Du, Rui Wang,* Ya-Ru Lv, Yong-Li Wei, Shuang-Quan Zang*

College of Chemistry and Molecular Engineering Zhengzhou University Zhengzhou 450001, China

Experimental section

Materials: All chemicals used in the experiment were purchased commercially and without further purification, which included cobalt nitrate hexahydrate ($Co(NO_3)_2{\cdot}6H_2O$, 99%), 1,3-bis(4-pyridyl)propane (bpp, 97%), 2,5-thiophenedicarboxylic acid (H_2tda, 98%), commercial RuO_2 (99.9%) and Pt/C (Pt 20 wt.%), N,N-Dimethylformamide (DMF), deionized water. All the solvents used were in analytical grade.

Synthesis of Co-NSOMOF: Co-NSOMOF was prepared with the improved method according to the literature.[19] $Co(NO_3)_2{\cdot}6H_2O$ (0.435 g), 2,5-thiophenedicarboxylic acid (0.1721 g), 1,3-bis(4-pyridyl)propane (0.1982 g) were dissolved in 30 mL N,N-dimethylformamide (DMF) under room temperature with stirring for 2 h. Then the mixture was refluxed for 12 h at 120 °C to form the purple precipitates. The resulting product was collected by centrifugation and washed with water and ethanol several times, followed by drying at 60 °C overnight.

Synthesis of Co/Co_9S_8@NSOC catalysts: The Co/Co_9S_8@NSOC catalysts were synthesized by the pyrolysis of Co-NSOMOF precursor. The Co-NSOMOF was placed in a tube furnace and calcined at various temperatures (600, 700, 800 and 900 °C) for 3 h under a flowing N_2 with a heating rate of 10 °C min^{-1}. After naturally falling to room temperature, the resulting products were treated in aqueous HCl solution for 6 h, followed by centrifugation and washed with deionized water and ethanol several times. Then the obtained products were dried at 60 °C for 12 h. The catalysts synthesized at different temperatures were named as Co/Co_9S_8@NSOC-T (T represents different pyrolysis temperatures).

Material characterization: The X-ray diffraction (XRD) patterns of the compounds were recorded on a Rigaku B/Max-RB X-ray diffractometer with Cu K_a radiation (λ=1.5418 Å). The X-ray photoelectron spectroscopy (XPS) measurements were carried out by ESCALAB 250 system (Thermo Electron) with an Al K_α (300 W) X-ray resource. The scanning electron microscope (SEM) measurements were performed using Zeiss Sigma 500. The transmission electron microscopy (TEM) images were obtained in FEI Tecnai G2 F20 S-TWIN electron microscope at an accelerating voltage of 200 kV. The Raman spectra were recorded on a LabRam HR Evolution. Nitrogen adsorption isotherms were measured at 77 K by using automatic volumetric adsorption equipment (Belsorp Max).

Electrochemical measurements: The electrochemical measurements were carried out with a typical three-electrode system by using CHI 660E electrochemical analyzer (CH Instruments Inc.). The Ag/AgCl (KCl, saturated) electrode and glassy carbon electrode coated with the as-prepared catalysts ink was used as the reference electrode and working electrode respectively. A graphite rod was used as the counter electrode (as considering that metal Pt will dissolve to some extent during the electrochemical cycling in electrolyte).[3, S1] The well-dispersed catalyst ink was prepared by dispersing 2 mg of the catalyst in 220 μL solution that containing 100 μL water, 100 μL DMF and 20 μL 5 wt.% Nafion solution, followed by ultrasonication for 30 minutes. Then, 5 μL of the catalyst ink was pipetted onto the glass-carbon electrode (GCE) with a catalyst loading of 0.64 mg cm^{-2}. The linear sweep voltammetry (LSV) curves were obtained at a scan rate of 5 mV s^{-1} in 1 M KOH solution. The chronoamperometric measurement of Co/Co_9S_8@NSOC-800 was conducted at a constant working potential for 10 h in 1 M KOH. The electrochemical impedance spectroscopy (EIS) measurements were carried out from 1000000 Hz to 0.1 Hz with an AC voltage amplitude of 5 mV. In all measurements, all the potentials were converted to the reversible hydrogen electrode (RHE) through RHE calibration: $E_{RHE} = E_{Ag/AgCl} + 0.197 + 0.059 \times pH$. The overpotential (η) was calculated according to the following formula:

OER: $\eta = E_{RHE} - 1.23$ V

HER: $\eta = E_{RHE} - 0$ V

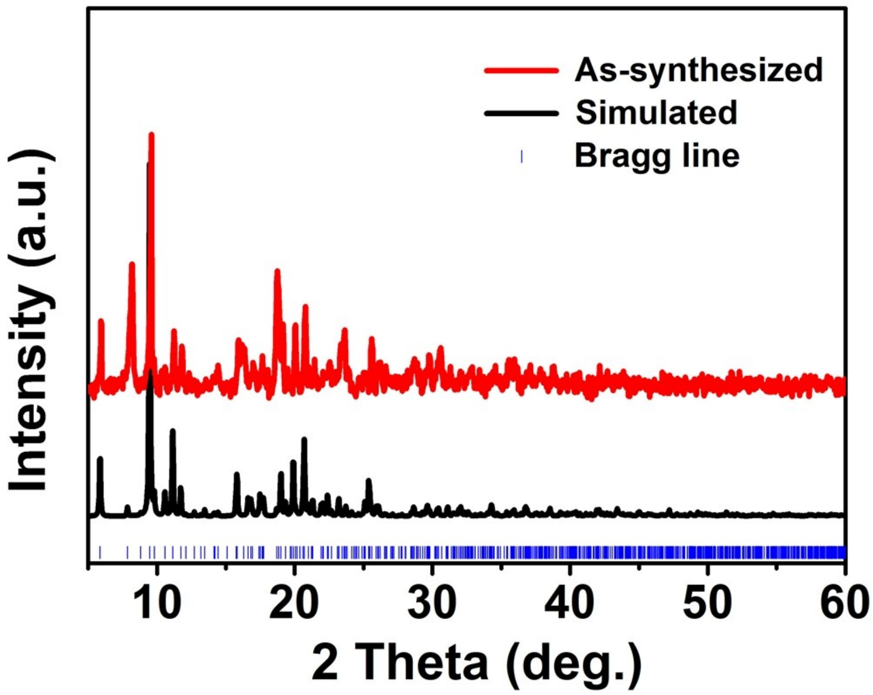

Fig. S1 PXRD pattern of as-prepared Co-NSOMOF. (Simulated pattern was obtained from the single-crystal data by the Mercury 1.8, CCDC number: 805455).

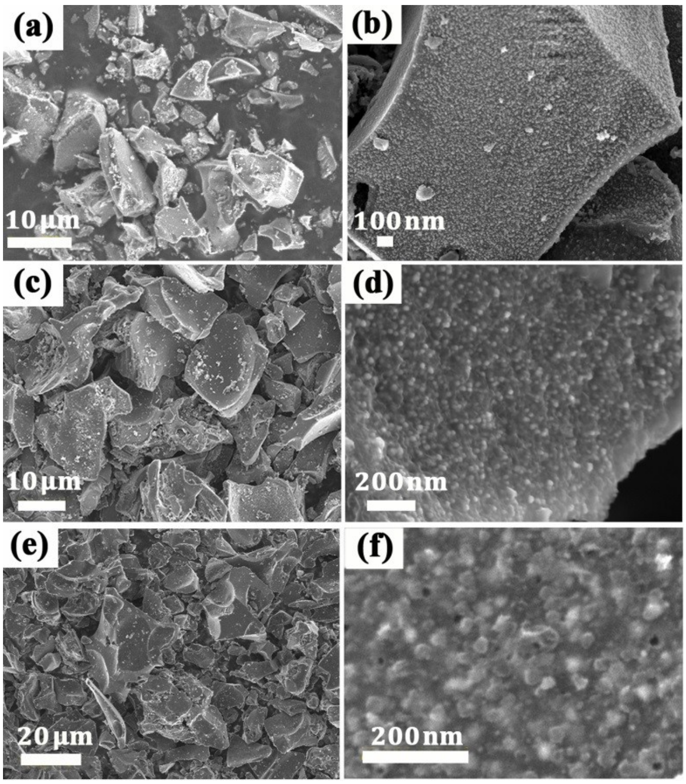

Fig. S2 SEM images of the (a, b) Co/Co_9S_8@NSOC-600; (c, d) Co/Co_9S_8@NSOC-700; (e, f) Co/Co_9S_8@NSOC-900.

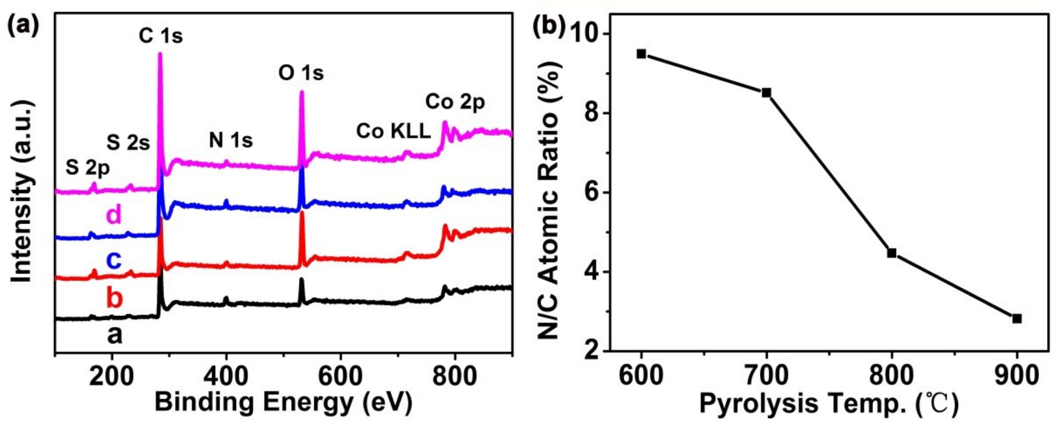

Fig. S3 XPS spectra and results based on the spectra for Co/Co_9S_8@NSOC materials. (a) XPS survey spectra. Lines a, b, c and d are Co/Co_9S_8@NSOC-600, Co/Co_9S_8@NSOC-700, Co/Co_9S_8@NSOC-800, and Co/Co_9S_8@NSOC-900; (b) N/C atomic ratios of Co/Co_9S_8@NSOC-T materials.

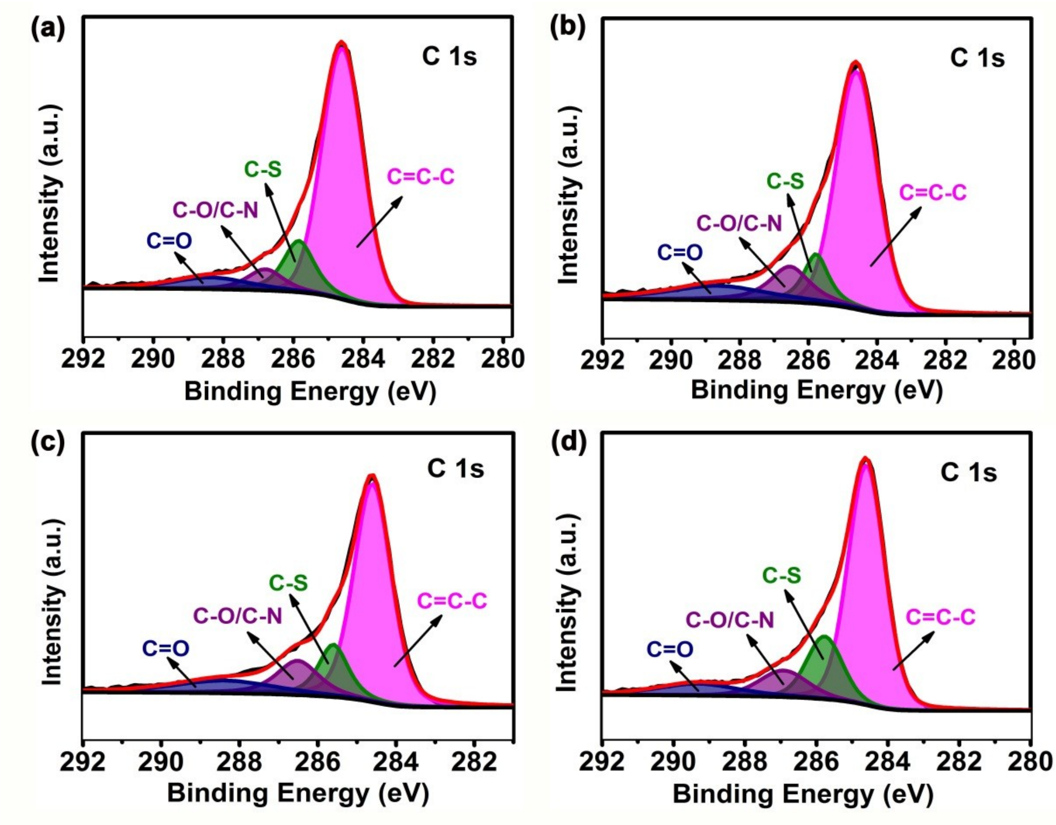

Fig. S4 High-resolution XPS spectra of C 1s for (a) Co/Co_9S_8@NSOC-600; (b) Co/Co_9S_8@NSOC-700; (c) Co/Co_9S_8@NSOC-800; (d) Co/Co_9S_8@NSOC-900.

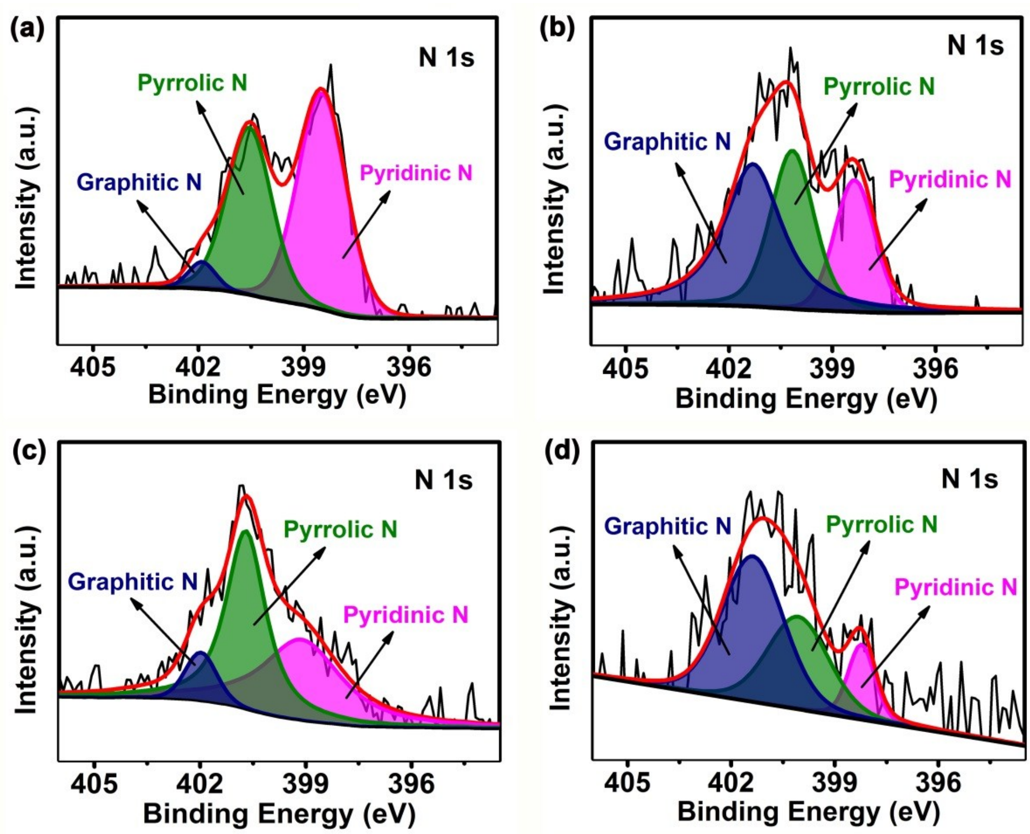

Fig. S5 High-resolution XPS spectra of N 1s for (a) Co/Co_9S_8@NSOC-600; (b) Co/Co_9S_8@NSOC-700; (c) Co/Co_9S_8@NSOC-800; (d) Co/ Co_9S_8@NSOC-900.

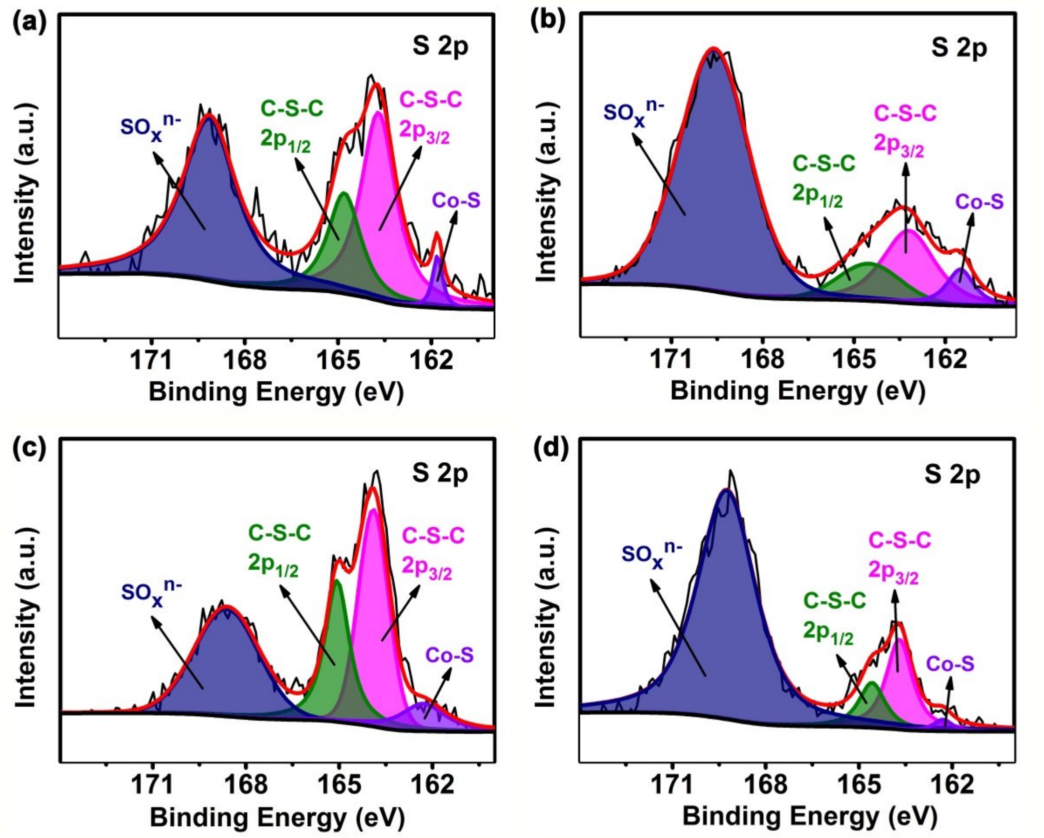

Fig. S6 High-resolution XPS spectra of S 2p for (a) Co/Co_9S_8@NSOC-600; (b) Co/Co_9S_8@NSOC-700; (c) Co/Co_9S_8@NSOC-800; (d) Co/ Co_9S_8@NSOC-900.

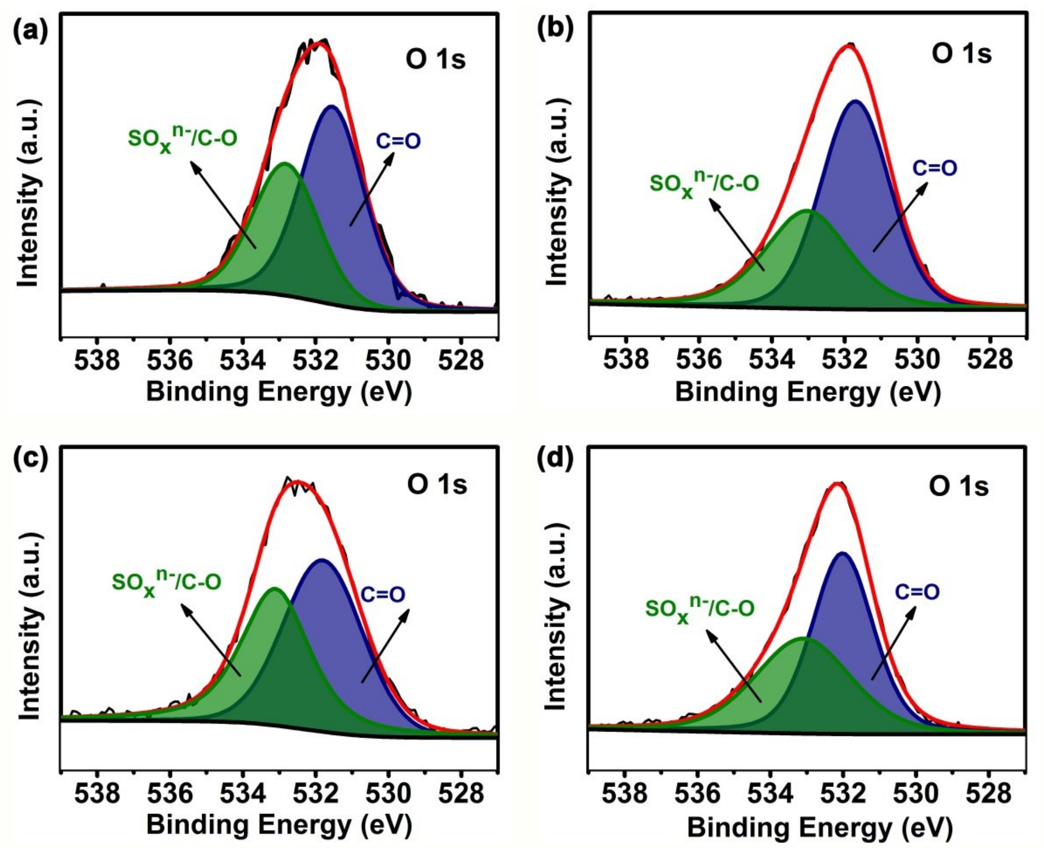

Fig. S7 High-resolution XPS spectra of O 1s for (a) Co/Co_9S_8@NSOC-600; (b) Co/Co_9S_8@NSOC-700; (c) Co/Co_9S_8@NSOC-800; (d) Co/Co_9S_8@NSOC-900.

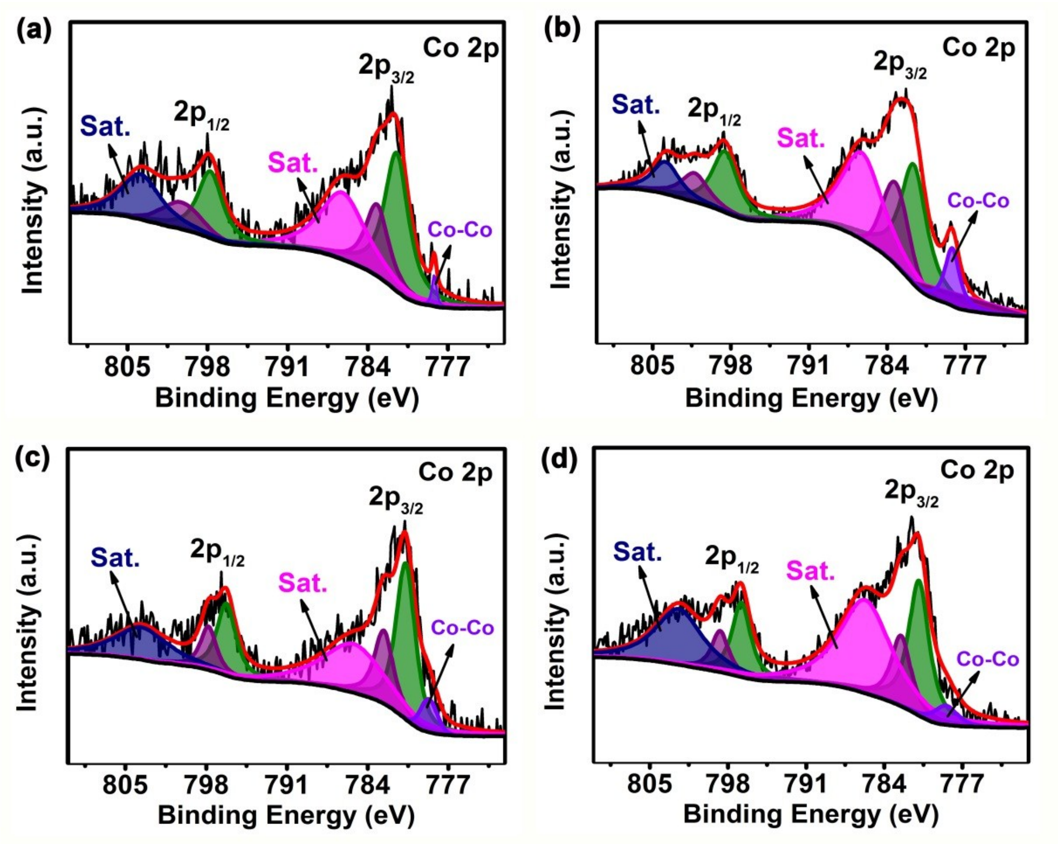

Fig. S8 High-resolution XPS spectra of Co 2p for (a) Co/Co_9S_8@NSOC-600; (b) Co/Co_9S_8@NSOC-700; (c) Co/Co_9S_8@NSOC-800; (d) Co/Co_9S_8@NSOC-900.

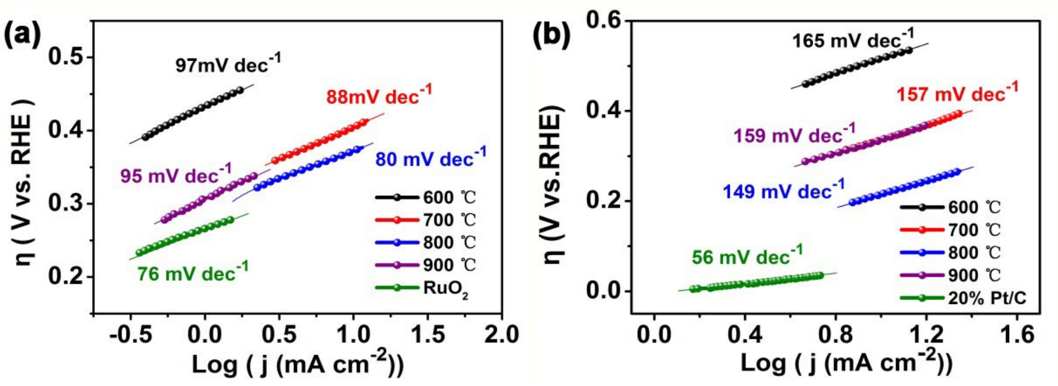

Fig. S9 (a) Tafel plots of Co/Co_9S_8@NSOC-T materials and RuO_2 for OER; (b) Tafel plots of Co/Co_9S_8@NSOC-T materials and Pt/C for HER.

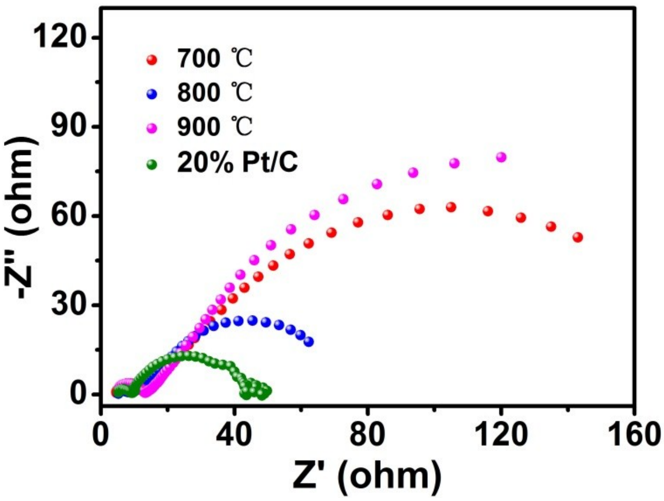

Fig. S10 Nyquist plots of the Co/Co_9S_8@NSOC-T and 20% Pt/C materials recorded at the frequency from 1000000 to 0.1 Hz at -0.227 V vs. RHE.

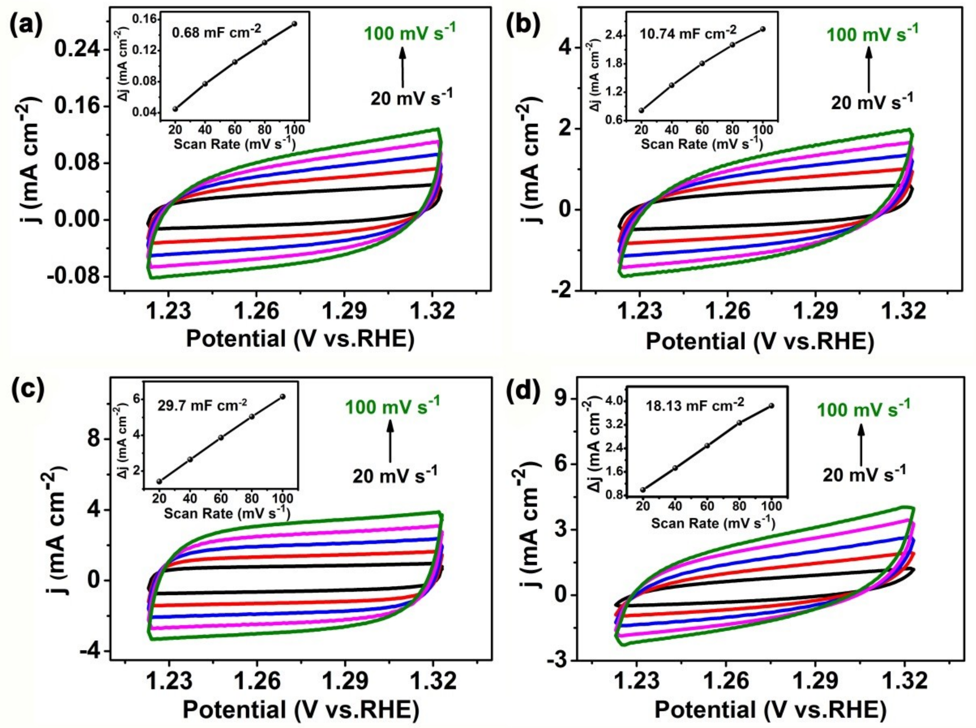

Fig. S11 Cyclic voltammograms (CVs) measured at various scan rates from 20 to 100 mV s^{-1} in the non-Faradaic region in 1 M KOH electrolyte. The materials are (a) Co/Co_9S_8@NSOC-600; (b) Co/Co_9S_8@NSOC-700; (c) Co/Co_9S_8@NSOC-800; (d) Co/Co_9S_8@NSOC-900; (inset: the corresponding scan rate dependence of the current density of Co/Co_9S_8@NSOC-600, 700, 800 and 900 respectively).

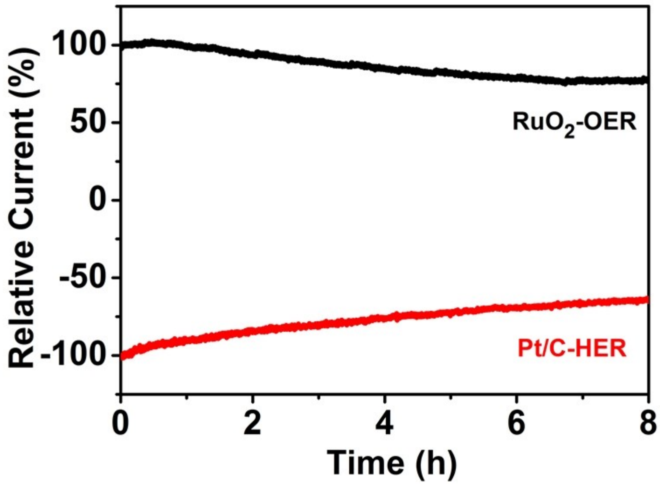

Fig. S12 The stability test of RuO_2 for OER and Pt/C for HER in 1 M KOH.

Note: As shown in Fig. S12, the relative current of commercial Pt/C for HER decreased to 64% and RuO_2 for OER decreased to 74% after 8 h continuous operation. And as shown in Fig. 3d, the relative current of Co/Co_9S_8@NSOC-800 were well maintained after 10 h continuous operation for both OER and HER, indicating that the electrochemical stability of Co/Co_9S_8@NSOC-800 was better than that of RuO_2 and Pt/C.

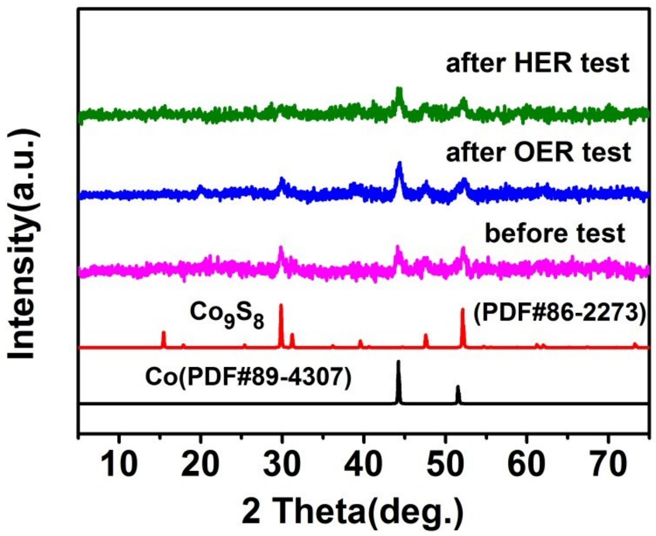

Fig. S13 PXRD patterns of the Co/Co_9S_8@NSOC-800 before and after 10 h chronoamperometry test for OER and HER.

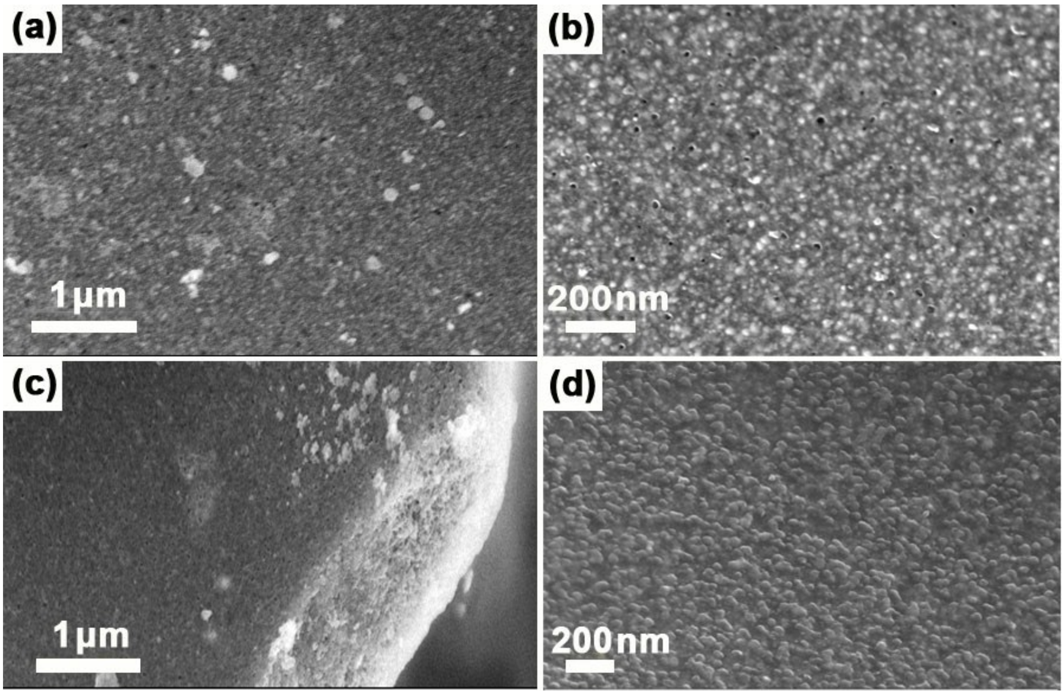

Fig. S14 SEM images of the Co/Co_9S_8@NSOC-800 before and after 10 h chronoamperometric test. (a, b) after OER long-term stability test; (c, d) after HER long-term stability test.

Table S1. Specific surface area and total pore volume of the Co/Co_9S_8@NSOC materials at different temperatures.

Sample	BET surface area (m^2 g^{-1})	Pore volume (cm^3 g^{-1})
Co/Co_9S_8@NSOC-600	2.3	0.01
Co/Co_9S_8@NSOC-700	38.7	0.05
Co/Co_9S_8@NSOC-800	96.4	0.16
Co/Co_9S_8@NSOC-900	64.2	0.13

Table S2. Comparison of HER and OER activity data of Co/Co_9S_8@NSOC-T materials.

Catalyst	Reaction	$\eta_{j=10mA\ cm^{-2}}$ [V]	Tafel slope [mV dec^{-1}]	C_{dl} [mF cm^{-2}]	R_{ct} [Ω]
600 °C	OER	0.530	97	0.68	648
	HER	0.517	165		
700 °C	OER	0.421	88	10.74	161
	HER	0.336	157		
800 °C	OER	0.373	80	29.70	23
	HER	0.216	149		
900 °C	OER	0.395	95	18.13	135
	HER	0.310	159		

Table S3. Comparison of electrocatalytic OER and HER performance of Co/Co_9S_8@NSOC-800 with other nonnoble metal electrocatalysts in the literatures.

Catalyst	OER $\eta_{j=10mA\ cm^{-2}}$ [mV]	Electrolyte	HER $\eta_{j=10mA\ cm^{-2}}$ [mV]	Electrolyte	Ref
Co_9S_8@MoS_2/CNFs	430	1 M KOH	190	0.5 M H_2SO_4	S2
Co_3S_4	363	1 M KOH	290	1 M KOH	S3
Co/CoO/$CoFe_2O_4$	330	1 M KOH	365	1 M KOH	S4
CoS_x@MoS_2	347	1 M KOH	239	0.5 M H_2SO_4	S5
Co_9S_8@NPC-10	403	1 M KOH	261	1 M KOH	6
Co-S/CP	363	1 M KOH	357	1 M KOH	S6
Co_xS_y@C-1000	470	0.1 M KOH	——	——	S7
PO-Ni/Ni-N-CNFs	420	1 M KOH	262	1 M KOH	S8
Ni_3S_2	400	1 M KOH	300	1 M KOH	S9
Co/Co_9S_8@NSOC-800	373	1 M KOH	216	1 M KOH	This Work

Table S4. Comparison of overall water splitting electrolysis cell performance of Co/Co_9S_8@NSOC-800 with other nonnoble metal electrocatalysts in the literatures.

Catalyst	$E_{j=10mA\ cm^{-2}}$ vs. RHE	Ref
CoP	1.62	S10
Co_3O_4	1.63	S11
Ni_2P	1.63	S12
Co_9S_8-NSC@Mo_2C/NF	1.61	S13
$Co_{0.9}S_{0.58}P_{0.42}$	1.59	S14
Co_9S_8	1.60	10
Cu@CoFe LDH-60	1.681	S15
Co_4Ni_1P	1.59	1
O-CoMoS	1.60	S16
PO-Ni/Ni-N-CNFs	1.69	S8
Co/Co_9S_8@NSOC-800	1.56	This Work

References

[S1] G. Dong, M. Fang, H. Wang, S. Yip, H. Y. Cheung, F. Wang, C. Y. Wong, S. T. Chu, J. C. Ho, *J. Mater. Chem. A*, 2015, **3**, 13080-13086.

[S2] H. Zhu, J. Zhang, R. Y. Zhang, M. Du, Q. Wang, G. Gao, J. Wu, G. Wu, M. Zhang, B. Liu, J. Yao, X. Zhang, *Adv. Mater.*, 2015, **27**, 4752-4759.

[S3] Z. F. Huang, J. Song, K. Li, M. Tahir, Y. T. Wang, L. Pan, L. Wang, X. Zhang, J. J. Zou, *J. Am. Chem. Soc.*, 2016, **138**, 1359-1365.

[S4] J. Y. Wang, C. Cui, R. B. Lin, C. H. Xu, J. Wang, Z. Q. Li, *Electrochimica Acta*, 2018, **286**, 397-405.

[S5] L. Yang, L. Zhang, G. Xu, X. Ma, W. Wang, H. Song, D. Jia, *ACS Sustainable Chem. Eng*., 2018, **6**, 12961-12968.

[S6] J. Wang, H. X. Zhong, Z. L. Wang, F. L. Meng, X. B. Zhang, *ACS Nano*, 2016, **10**, 2342-2348.

[S7] P. Zeng, J. Li, M. Ye, K. Zhuo, Z. Fang, *Chem. Eur. J.*, 2017, **23**, 9517-9524.

[S8] Z. Y. Wu, W. B. J, B. C. Hu, H. W. Liang, X. X. Xu, Z. L. Yu, B. Y. Li, S. H. Yu, *Nano Energy*, 2018, **51**, 286-293.

[S9] T. A. Ho, C. Bae, H. Nam, E. Kim, S. Y. Lee, J. H. Park, H. Shin, *ACS Appl. Mater. Interfaces*, 2018, **10**, 12807-12815.

[S10] Y. P. Zhu, Y. P. Liu, T. Z. Ren, Z. Y. Yuan, *Adv. Funct. Mater.*, 2015, **25**, 7337-7347.

[S11] P. Z. Yun, Y. M. Tian, M. Jaroniec, Z. Q. Shi, *Angew. Chem. Int. Ed.*, 2017, **56**, 1324-1328.

[S12] L. A. Stern, L. Feng, F. Song, X. Hu, *Energy Environ. Sci.*, 2015, **8**, 2347-2351.

[S13] H. Zhu, J. Zhang, R. Yanzhang, M. Du, Q. Wang, G. Gao, J. Wu, G. Wu, M. Zhang, B. Liu, J. Yao, X. Zhang, *Adv. Mater.*, 2015, **27**, 4752-4759.

[S14] Z. Dai, H. Geng, J. Wang, Y. Luo, B. Li, Y. Zong, J. Yang, Y. Guo, Y. Zheng, X. Wang, Q. Yan, *ACS Nano*, 2017, **11**, 11031-11040.

[S15] L.Yu, H. Q. Zhou, J. Y. Sun, F. Qin, D. Luo, L. X. Xie, F. Yu, J. M. Bao, Y. Li, Y. Yu, S. Chen, Z. F. Ren, *Nano Energy*, 2017, **41**, 327-336.

[S16] J. G. Hou, B. Zhang, Z. W. Li, S. Y. Cao, Y. Q. Sun, Y. Z. Wu, Z. M. Gao, L. C. Sun, *ACS Catal.*, 2018, **8**, 4612-4621.